Optical design rules of a camera module with a liquid lens and principle of command for AF and OIS functions

Eric Simon*, Bruno Berge*, Franck Fillit, Hilario Gaton, Martin Guillet, Olivier Jacques-Sermet, Frédéric Laune, Julien Legrand, Mathieu Maillard, Nicolas Tallaron
Varioptic, 24B, rue Jean Baldassini, 69007 Lyon, France

ABSTRACT

We have developed a miniature liquid lens component based on electro-wetting. It is designed to be plugged on a fix focus camera module lens to provide both optical image stabilization (OIS) and auto-focus (AF) functions without any mobile mechanical parts. The OIS/AF liquid lens component features a conical shape supporting the liquid interface in order to maintain a stable optical axis and a multi-electrode design able to induce an average tilt of the liquid interface when a bias voltage is applied to the different electrodes. The miniature size of the OIS/AF liquid lens component is well adapted to imaging applications with ¼ inch, 1/3 inch and possibly 1/2.5 inch sensor formats. We will present general rules for the optical design with an OIS/AF liquid lens. In this context, we will describe a simple calculation, based on the well known Maréchal criterion, to estimate the optical wave front error requirement of an optical component positioned in the aperture stop plane of an imaging lens design to perform images with a pixel resolution quality. We will also present the principle of command of a multi-electrode liquid lens in order to perform AF and OIS functions with an optimal image quality.

Keywords: Liquid lens, optical image stabilization, OIS, optical beam tuner

*eric.simon@varioptic.com ; bruno.berge@varioptic.com

1. INTRODUCTION

The camera phone evolution is to increase pixel count, while maintaining small sensor formats for overall size constraints. The pixel shrinking has led to degrade light sensitivity and to increase the pictures exposure time. The image quality of most of the indoor pictures taken with high resolution miniature camera modules of cellular phones is limited by the handshake blur[1]. Several groups have been pointing this major problem in mobile imaging, which can only be resolved by an Optical Image Stabilization system[2]. Among the different OIS technologies under development[3], a liquid lens component based on electro-wetting[4,5] can generate an electrically controlled optical tilt in two directions with a tilt range and a response time well adapted to the design of an OIS on a miniature mobile phone camera module. Liquid lens actuated by electro-wetting is composed of a cell filled of two immiscible liquids with the same density, realizing a very robust and acceleration independent device, while keeping its flexibility for fast changes of liquid interface shape. It brings an optical component presenting the best compromise between low actuator forces, focusing range, tilt range and roughness. An OIS liquid lens can also provide focus control[6] and enable the realization of a miniature OIS auto-focus (AF) camera module without any mobile mechanical parts. In this paper, we present the OIS/AF liquid lens principle and we describe an example of implementation in a camera module. We explain the principles of the electrical commands of optical focus and optical tilt. We present a rule of thumb for performing optical design with a liquid lens and we give some examples of reference designs of miniature camera modules with liquid lens. At the end of the paper we list some possible applications for the OIS liquid lens component.

2. OIS/AF LIQUID LENS: PRINCIPLE AND OVERALL DESCRIPTION

The liquid lens is composed of two liquids, one is electrically insulating like oil, and the other one is an electrolyte. They have substantially the same density to prevent from linear acceleration effect and a refractive index difference Δn, to form an optical interface having an optical power of $1/f = \Delta n/R$ with R the curvature radius of the liquid interface. These two liquids are standing on a hydrophobic and dielectric coating of parylene C, forming a triple interface characterized by a contact angle α. When voltage is applied to the dielectric coating, the wettability of liquids is modified due to charge density modification at the interface between the dielectric coating and the liquids. In the case of a drop of non conducting liquid, surrounded by a conducting liquid, electro-wetting phenomenon is fairly well described by the following equation[5,7]:

$$Cos\,\alpha = Cos\,\alpha_0 - \frac{\varepsilon\varepsilon_0}{2d\gamma}V_{RMS}^2 \qquad (1)$$

with α_0 the natural contact angle (as measured without applied voltage) between the oil and the surface, ε the dielectric constant of the dielectric layer, ε_0 the permittivity of vacuum, d the dielectric thickness, γ the interface tension and V_{RMS} the rms value of the applied voltage. This equation remains valid as long as the voltage does not exceed the saturation voltage[7]. In liquid lens technology, applied voltage is an AC voltage having a frequency between 1 and 5kHz, and a zero voltage average (<V>=0) to prevent from charge injection in the dielectric coating. As described by the electro-wetting equation, contact angle from the non-conducting droplet is thus increasing with applied voltage. This phenomenon is highly reversible with low hysteresis with properly designed liquids and coating, namely liquids having a low contact angle when no voltage is applied[8]. In a liquid lens, the oil droplet is spatially confined in a conical cavity and acts as a lens having a variable focal length, depending on the contact angle and the applied voltage consequently, (see figure1).

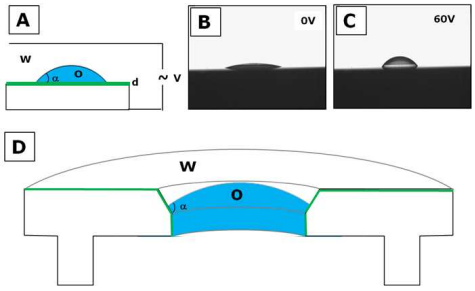

Figure 1. A: schematic principle of electro-wetting involving a drop of oil (o) having a contact angle α on an insulating coating (green) of thickness d, surrounded by a conducting fluid (w) - B and C: images of the same oil drop on a parylene coating at 0 and 60V rms (1kHz sinus) - D: schematic view of the lower part of a liquid lens, including the dielectric coating (green), the oil drop confined in the conical cavity. (o) and the conducting liquid (w).

The conical shape is insuring a restoring force for the liquid interface to come at the center position[6]. When the same voltage is applied on the whole surface of the dielectric coating, liquid interface has the same contact angle at every point of the contact line and the shape of the liquid interface remains both spherical and centered on the conical cavity symmetry axis. When multiple electrodes are used to apply differential voltages on the dielectric coating, see figure 2, multiple contact angle are available along the contact line, allowing complex liquid interface shape and thus more complex optical functions like astigmatism or tilt depending on the voltage profile. The principle of OIS lens driving is explained in more details in the section 4. The optical performances of A316S OIS liquid lens component are summarized in the table 1 below and presented in more details in a previous publication[9].

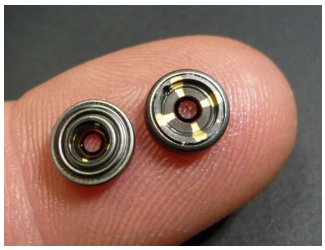

Figure 2. A316S OIS liquid lens with 4 electrodes

Table 1. A316S – OIS liquid lens main features

Item	Value
Optical transmission	>95%
Optical tilt range	+/-0.6°
Full range tilt response time @ 25°C	30ms @ 90% of the full tilt command
Focus range	0 to 15 diopters
Optical wave front error in AF mode	See Equation 12
Optical wave front error in OIS mode (focus range for OIS is 0 to 5 diopters)	<50nm-rms/0.1° over 1.6mm diameter
Operating temperature	From -10°C to 60°C
Storage temperature	From -40°C to 85°C

3. OIS/AF CAMERA MODULE WITH A LIQUID LENS

A fix focus camera module can be simply transformed into an AF/OIS camera module with the implementation of a liquid lens component. The liquid lens is mechanically plugged onto the fix focus camera lens of a camera module (add-on design) and it is electrically connected to the command board with a flexible printed circuit board (PCB). The auto-focus adjustment of the camera module can be obtained with a closed loop command of the optical power of the liquid lens from an estimation of the sharpness of the image by the image processor. The principle of optical image stabilization consists in measuring the instantaneous handshake tilt of the camera module with a two axis gyroscope and generating an opposite tilt with the liquid lens. A theoretical estimation of the efficiency of OIS with a liquid lens has been presented in a previous publication[10]. We have developed a small electronic set-up board enabling to evaluate experimentally the image quality, the focus control and the OIS performances. The experimental set-up includes a sensor control board with an image processing, an A316S OIS liquid lens maintained on the camera module with a compression spring and a liquid lens control board including a dual-axis gyroscope, a signal post processing microcontroller and a liquid lens driver. The driving circuitry of the OIS liquid lens is very compact due to the availability of a specific integrated driver from Maxim Integrated Products, see. Figure 3. We show on video 1 an example of a film taken with our experimental set-up to illustrate the efficiency of a real time tilt correction that can be performed by the A316S OIS liquid lens.

Figure 3.Liquid lens and driver MAX14574EWL+ with external components

Video 1. Example of optical image stabilization performed with A316s liquid lens on a vibrating table. Tilt amplitude: +/-0.5°; Frequency: 4Hz. A316s_OIS_video**http://dx.doi.org/doi.number.goes.here**

4. OIS LENS DRIVING.

4.1 Principle of liquid lens driving

The curvature and the tilt of the optical diopter formed by the two liquids of the liquid lens are controlled by the addition of a uniform voltage V_0 and a non uniform voltage varying as a function of the azimuth angle ϕ along the cone, see figure 4. The optical tilt θ_{opt} induced by a geometrical tilt θ_{liqu} of the liquid interface depends on the optical index of the two liquids and can be simply expressed with the Snell-Descartes refraction law.

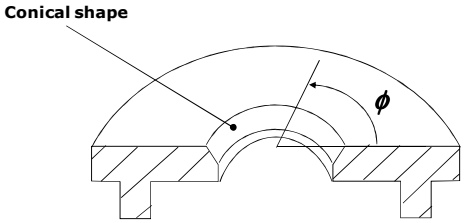

Figure 4: Definition of the azimuth angle ϕ along the cone.

The curvature of the spherical interface between the two liquids is imposed by a uniform voltage component V_0 applied on the cone[6] which generates a homogenous angle α_{V0} between the liquids interface and the cone according to the equation 1. When the liquid interface is tilted, the angle between the liquid interface and the cone $\alpha(\phi)$ depends on the azimuth angle. The difference $\alpha(\phi) - \alpha_{V0}$ is obtained by the application of an additional non-uniform voltage along the cone. The theoretical non –uniform voltage $V_{theo}(\phi)$ required to create a tilt θ_{liqu} of the liquid interface along an azimuth direction ϕ_0 can be expressed with equation (1) on the basis of a geometrical estimation of the local angle $\alpha(\phi)$ between a sphere and the cone surface as a function of the azimuth. When the liquid interface is plane, the expression of $\alpha(\phi)$is simply given by the following equation:

$$\alpha(\phi) = \alpha_{V0} + \theta_{liqu} \cdot \cos(\phi - \phi_0) \qquad (2)$$

Practically, the combination of a uniform voltage V_0 and a non uniform voltage along the cone is obtained with a design featuring 4 electrodes and a resistive layer between the electrodes. The common electrode is the metal cap of the lens. When 4 different voltages $V_{x+}(t)$, $V_{y-}(t)$, $V_{x-}(t)$, $V_{y+}(t)$ are respectively applied on the 4 electrodes, the instantaneous voltage $V(\phi,t)$ along the cone is linearly variable from an electrode to another. The application of a DC voltage on the liquid lens is not possible because of polarization effects on the cone. For this reason, the 4 voltage commands $V_{x+}(t)$, $V_{y-}(t)$, $V_{x-}(t)$, $V_{y+}(t)$ are modulated at a frequency of a few KHz. The modulation frequency is significantly higher than the focus and the tilt response time of the liquid lens so that it has no impact on the optical characteristics of the liquid lens. The calculation of the rms voltage along the azimuth of the cone depends on the waveform of the voltages applied on the electrodes $V_{x+}(t)$, $V_{y-}(t)$, $V_{x-}(t)$, $V_{y+}(t)$. In case if the four voltages are synchronously amplitude modulated, the evaluation

of the rms voltage $V_{AM\text{-}rms}(\phi)$ is similar to the evaluation of the instantaneous voltage $V(\phi,t)$: upon the 4 electrodes, $\phi = 0°$, $\phi = 90°$, $\phi = 180°$and $\phi = 270°$ the values of $V_{AM\text{-}rms}(\phi)$ are respectively the rms values $V_{x+\ rms}$, $V_{y-\ rms}$, $V_{x-\ rms}$, $V_{y+\ rms}$ of $V_{x+}(t)$, $V_{y-}(t)$, $V_{x-}(t)$, $V_{y+}(t)$ and the voltage $V_{AM\text{-}rms}(\phi)$ is linearly variable from an electrode to another. We show on figure 5 a calculation of $V_{theo}(\phi)$ and $V_{AM\text{-}rms}(\phi)$ with a voltage $V_0 = 50V$ corresponding to plan interface (0 diopter) and with a non-uniform voltage component corresponding to an optical tilted $\theta_{opt} = 0.5°$ along the along the azimuth direction $\phi_0 = 0°$. For power consumption optimization, it is interesting to drive the electrodes with 4 Pulse Width Modulation (PWM) signals. In that case, the values of $V_{PWM\text{-}rms}(\phi)$ are respectively $V_{x+\ rms}$, $V_{y-\ rms}$, $V_{x-\ rms}$, $V_{y+\ rms}$ upon the 4 electrodes, but $V_{PWM\text{-}rms}(\phi)$ is not anymore simply linearly variable from an electrode to another. We show on figure 4 a calculation of $V_{PWM\text{-}rms}(\phi)$ obtained for an optical focus of 0 diopter and an optical tilt $\theta_{opt} = 0.5°$, assuming a synchronous bipolar PWM signal with a peak voltage of 70V.

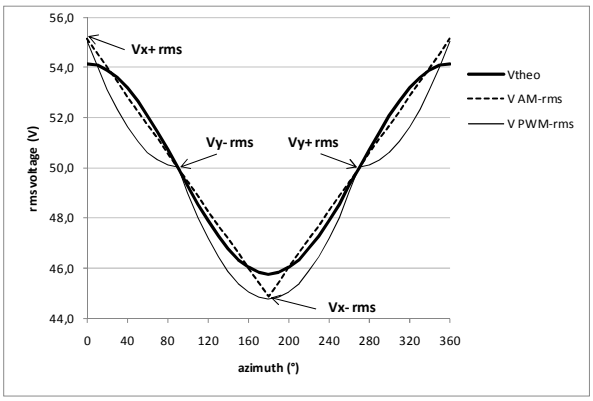

Figure 5. Voltage along the azimuth of the cone: theoretical value and rms values with a four electrode design with AM or PWM signals

Based on equation (1) and equation (2), a Fourier decomposition of the difference between the real signal $V_{PWM\text{-}rms}(\phi)$ and the theoretical signal $V_{theo}(\phi)$ enables to estimate the optical wave-front aberration contributors in a Zernike polynomial decomposition. The average value of $V_{PWM\text{-}rms}(\phi) - V_{theo}(\phi)$ over $[0, 2\pi]$ induces a defocus and the $\cos(n\ \phi)$ and $\sin(n\ \phi)$ harmonics of $V_{PWM\text{-}rms}(\phi) - V_{theo}(\phi)$, for $n>1$, generate an optical wave front error respectively proportional to Z_n^n and Z_n^{-n} Zernike polynomial[11]. We show in the table 2 the Zernike polynomials corresponding to the first Fourier harmonic of the difference $V_{PWM\text{-}rms}(\phi) - V_{theo}(\phi)$.

Table 2. A316S – Optical aberration generated by the harmonic of the voltage error for a tilt command

Fourier harmonic of $(V_{PWM\text{-}rms} - V_{theo})(\phi)$	**Corresponding optical wave-front aberration**	**Zernike Polynomial**
Constant	**defocus**	Z_2^0
$\cos(\phi)$	**Tilt along** ϕ_0**=0°**	Z_1^1
$\sin(\phi)$	**Tilt along** ϕ_0**=90°**	Z_1^{-1}
$\cos(2\phi)$	**Astigmatism along** ϕ_0**=0°**	Z_2^2
$\sin(2\phi)$	**Astigmatism along** ϕ_0**=45°**	Z_2^{-2}
$\cos(3\phi)$	**Trefoil along** ϕ_0**=0°**	Z_3^3
$\sin(3\phi)$	**Trefoil along** ϕ_0**=30°**	Z_3^{-3}
$\cos(4\phi)$	**Tetrafoil along** ϕ_0**=0°**	Z_4^4
$\sin(4\phi)$	**Tetrafoil along** ϕ_0**=22.5°**	Z_4^{-4}

The analysis of the rms optical wave-front error generated with a PWM signal for different amplitudes and directions of tilt shows that the wave-front error depends on the direction of the tilt, that it is proportional to the tilt amplitude and that 90% of the rms wave-front error is due to defocus, astigmatism and trefoil. The size of the electrode can influence the wave front error pattern. In figure 5, we made the assumption that the electrode size was negligible. With a PWM signal, the defocus induced during a tilt due to the variation of the average value of the difference $V_{\text{PWM-rms}}(\phi)$ - $V_{\text{theo}}(\phi)$ over [0, 2π] is a predominant term, see figure 5. It is possible to make this term negligible with a correction law adjusting the average value of $V_{\text{PWM-rms}}(\phi)$ - $V_{\text{theo}}(\phi)$ close to zero for all the possible tilt command. We give below an example of a matrix command for the 4 electrode voltages of the A316S lens with PWM signals such as those generated by the quad-driver MAX14574EWL+ from Maxim Integrated Products. This matrix command includes a correction law reducing the focus and tilt cross talk by a factor of 10:

$$\begin{bmatrix} V_{x+} \\ V_{x-} \\ V_{y+} \\ V_{y-} \end{bmatrix} = V_0 \cdot \begin{bmatrix} 1 \\ 1 \\ 1 \\ 1 \end{bmatrix} + \begin{pmatrix} +G_{tilt} & 0 & \varepsilon \\ -G_{tilt} & 0 & \varepsilon \\ 0 & +G_{tilt} & \varepsilon \\ 0 & -G_{tilt} & \varepsilon \end{pmatrix} \cdot \begin{bmatrix} \theta_x \\ \theta_y \\ |\theta_x - \theta_y| + |\theta_x + \theta_y| \end{bmatrix} \qquad (3)$$

With:

$$\begin{pmatrix} \theta_x \\ \theta_y \end{pmatrix} = \theta_{opt} \cdot \begin{pmatrix} \cos(\phi_0) \\ \sin(\phi_0) \end{pmatrix} \qquad (4)$$

The focus is set by changing the 4 electrode voltages at the same time at a given value V_0. Once the focus voltage is set, the voltage variation on each electrode with respect to previous matrix provides the tilt. The term G_{tilt} describes the linear dependence between an optical tilt and a voltage offset between opposite electrodes. The term ε is a parameter of the focus correction law specific to the PWM signals. For tilt commands with amplitudes smaller that 0.1°, the rms wave-front error over a 1.6mm diameter useful optical aperture is of the same order of magnitude as the wave-front error limit in AF mode and it is mainly due to random irregularity of the electrical and mechanical features of the cone. For tilt commands with amplitudes higher than 0.1°, the rms wave-front error over a 1.6mm diameter useful optical aperture is mainly due to the astigmatism and to the trefoil and it remains smaller than 50nm/0.1° in any tilt directions. We show in figure 6 the rms wave-front error measured with a liquid lens sample over a 1.6mm diameter for 8 different tilt configurations. We use the matrix command described in equation (3): the optical tilt amplitude is 0.4° and the azimuth directions of the tilt start from ϕ_0 = 0° and are regularly spaced of 45°.

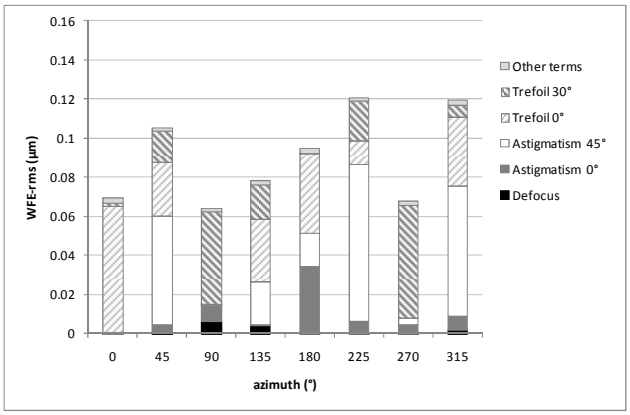

Figure 6.Wavefront error measurement of an OIS liquid lens over a 1.6mm diameter for a 0.4° tilt amplitude along 8 different directions

4.2 Tilt response time optimization

The tilt response time of the lens presented in table 1 can be improved by applying an over voltage during a controlled time. This driving process can be done by applying a specific overshoot filter to the tilt command signal in order to accelerate the tilt of the oil drop. We illustrate in figure 7 the tilt response acceleration obtained with a linear second-order pass band filter.

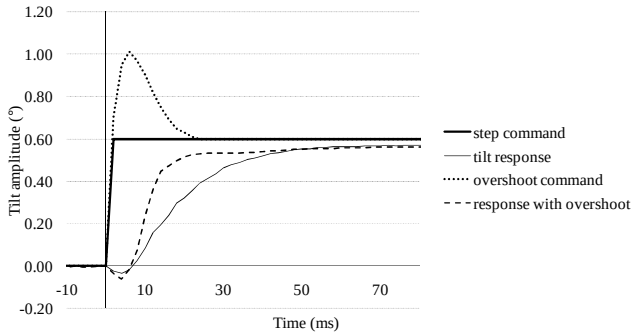

Figure 7.Comparison of the tilt response of the A316S OIS liquid lens with and without overshoot command.

The effect of this overshoot is particularly interesting at low temperature because the viscosity of the liquids is more important and the tilt response time of the lens is reduced. An optimal tilt response time of the liquid lens over the whole operational temperature range of the camera can be obtained with a coarse linear adjustment of the gain of the filter as a function of the liquid lens temperature. The improvement of the blur correction using this filter has been evaluated on an OIS system described in figure 8 with different handshake movements.

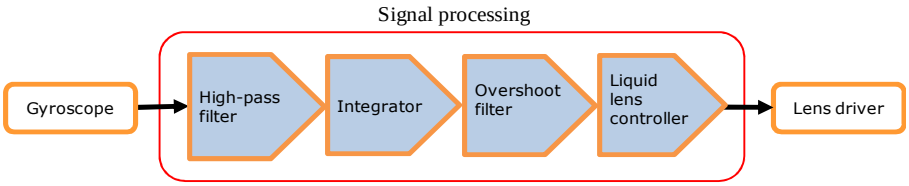

Figure 8. Schematic of an OIS gyroscope signal processing with overshoot filter

The efficiency depends of the kind of movement but the result is always positive. The figure 9 shows an example of tilt accuracy improvement on a recorded real handshake signal with the overshoot filter:

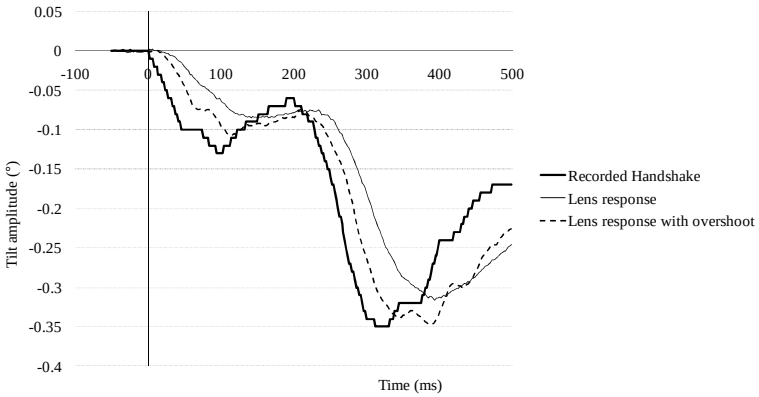

Figure 9: Comparison of tilt response accuracy on one axis with and without overshoot filter.

5. IMAGE QUALITY AND OPTICAL WAVE FRONT ERROR

5.1 Introduction

The AF/OIS liquid lens is a modular component which can be simply plugged on several existing camera module designs. Due to the relatively low optical power of the liquid lens, the relative centering of the liquid lens within the camera lens is not a critical parameter of the optical design. One important parameter is the optical wave-front error induced on the camera lens by the liquid lens. The optical wave front-error of the liquid lens is due to non-homogeneities of the cone surface or of the electrical field along the cone. We present below rules of thumb enabling a rapid evaluation of the feasibility of the implementation of a liquid lens on a given fix focus camera module with an optimal image quality. We perform an estimation of the optical wave-front error requirement of the liquid lens, which is based on an extrapolation of the Maréchal criterion from diffraction limited optical systems to pixel resolution limited imaging systems. We extend this estimation to OIS systems.

5.2 Wave front error requirement for a pixellated imaging system.

André Maréchal[12] has shown in 1946 that an optical imaging system could perform optimal image resolution at a wavelength λ under the condition that the rms value of the optical wave front error - difference between the real optical wave-front and an ideal wave-front - is smaller than $\lambda/14$. An optical system meeting the Maréchal criterion is commonly given as diffraction limited. Today most of the imaging systems have an optoelectronic sensor with an array of pixels and the intrinsic limit of the image resolution is often due to the pixel spacing of the image sensor rather than to the diffraction spot size. The achievement of a camera with an optimal image quality doesn't necessarily require a diffraction limited camera lens. For a given optical wave-front pattern, the aberration spot size is proportional to the rms value of the wave-front error. As a consequence, the rms wave-front error requirement $WFE_{lens\text{-}rms}$ for a camera lens of an imaging system with a resolution intrinsically limited by the pixel spacing can be linearly expressed from the $\lambda/14$ rms wave-front error requirement of a diffraction limited system and from the ratio of the respective image resolution limit from the pixels and from the diffraction spot. The order of magnitude of this last ratio is the ratio of pixel spacing d_{pix} over the diffraction spot size $f\,\lambda/D$ where f is the focal distance of the camera lens and D the diameter of the aperture stop. A more accurate estimation of ratio of the image resolution limit from the pixels and from the diffraction spot can be given by the calculation the inverse ratio of the spatial frequency corresponding to a standard criteria of 50% loss of MTF for respectively a sensor array and for a perfect diffraction limited camera lens:

$$WFE_{lens-rms} < \frac{\lambda}{14} \cdot \frac{\nu_{50\%MTF-diffraction}}{\nu_{50\%MTF-sensor}}$$

$$or \qquad (5)$$

$$WFE_{lens-rms} < \frac{\lambda}{14}$$

The case when $\nu_{50\%MTF\text{-}sensor}$ is significantly higher than $\nu_{50\%MTF\text{-}diffraction}$ corresponds to a case when the diffraction spot is significantly larger than the sensor pixel spacing. With a perfect diffraction limited lens featuring a circular stop, the spatial frequency expressed in number of cycles per meter corresponding to 50% MTF and is given by[11]:

$$\nu_{50\%MTF-diffraction} = \frac{0.4}{f \cdot \lambda / D} \qquad (6)$$

For the MTF of array sensors, we use the calculation of a pseudo MTF assuming that all the phases of the pattern are equally likely in order to average the effect of the aliasing. The spatial frequency expressed in number of cycles per meter corresponding to 50% loss of MTF of an array sensor can be generally expressed with the following equation:

$$v_{50\%MTF-sensor} = \frac{k_{sensor}}{d_{pix}} \qquad (7)$$

The value k_{sensor} is depending on the geometry of the sensor pattern. The highest value can be obtained with an array sensor with square pixels and a filling factor of 100%. The value of k_{sensor} is significantly reduced with a color sensor array[13]. We give in the table below some value of k_{sensor} for different type of sensor array:

Table 3. Value of k_{sensor} constant for different types of sensors

Type of sensor	$\boldsymbol{k_{sensor}}$
Monochrome sensor with square pixels and ideal 100% filling factor	0.6
Color sensor with a Bayer pattern filter - square pixels with an ideal filling factor of 100%	0.28

From the equations (5), (6) and (7), we can simply express the WFE requirement as a function of the optical system *f* number, $N=f/D$ and as a function of the pixel spacing d_{pix} as follow:

$$WFE_{lens-rms} < \frac{1}{k_{sensor}} \cdot \frac{d_{pix}}{35 \cdot N} \qquad (8)$$

for a pixel limited resolution or

$$WFE_{lens-rms} < \frac{\lambda}{14} \text{ when } \frac{d_{pix}}{k_{sensor}} < 2.5 \cdot N \cdot \lambda \qquad (9)$$

for a diffraction limited resolution. With a classical color sensor with Bayer filter, the previous WFE requirement is:

$$WFE_{lens-rms} < \frac{d_{pix}}{10 \cdot N} \qquad (10)$$

for a pixel limited resolution or

$$WFE_{lens-rms} < \frac{\lambda}{14} \qquad (11)$$

for a diffraction limited resolution. The second term of equation (9) gives a simple evaluation of a sensor requirement for pixel spacing d_{pix} and k_{sensor} in order to perform image quality of the same order of magnitude as the diffraction limit of a perfect lens. We give in the table 4 below examples of wave-front error requirements estimated from equation (10) for the most standard color camera modules in the mobile phone context. Since inch-based sensor formats are not standardized, exact number of pixels may vary.

Table 4. Estimation of the wave-front error requirements for f/2.8 and f/4 camera lenses featuring a sensor array with a Bayer color filter:

Color camera module features			WFE requirement (µm)	
Pixel spacing (µm)	nb of Mpixel (4/3 format)	indicative optical format	f/2.8 aperture	f/4 aperture
1.4	5.0	1/4"	0.051	0.036
	7.9	1/3.2"		
	12.6	1/2.5"		
1.75	3.2	1/4"	0.064	0.045
	5.1	1/3.2"		
	8.1	1/2.5"		
2.2	2.0	1/4"	0.080	0.056
	3.2	1/3.2"		
	5.1	1/2.5"		
2.8	1.2	1/4"	0.102	0.071
	2.0	1/3.2"		
	3.2	1/2.5"		

5.3 Wave-front error requirement: application to the liquid lens

The wave-front error of the liquid lens is mostly induced at the interface between the two liquids. We have shown in figure 7 the Zernike polynomial decomposition of the wave-front error for the specific case of a 0.4° tilt applied on the liquid lens. When no optical tilt is applied (pure AF mode), we observe that the wave-front is mainly due to astigmatism and the estimation of the rms wave-front error magnitude induced by the liquid lens in an optical system can be expressed as a function of the useful optical diameter D_{use} at the interface between the two liquids as follow:

$$WFE_{rms-D} \approx WFE_{rms-1.6}\left(\frac{D_{use}}{1.6}\right)^2 \qquad (12)$$

D_{use} is expressed in unity of millimeter. With A316S OIS liquid lens component, the maximal value of D_{use} is 2.6mm and we guarantee $WFE_{rms\text{-}1.6} < 50$nm over a 1.6mm diameter and over the -5D to +15D optical power range[9].

The estimation of the feasibility of the implementation of a liquid lens in a camera module design with no degradation of the image quality can be performed from the equations (8) and (11) and from an estimation of the useful optical diameter at the liquids interface of the liquid lens. For an add-on design, with a given aperture and a given field of view, the best optical performances can be obtained with a value of D_{use} as small as possible. This can be obtained by positioning the liquid lens as close as possible to the aperture stop of the camera lens and it can be further improved with the implementation of the aperture stop of the optical system in the liquid lens. We have validated this option on A316S component with the implementation of an optional intra-pupil on the inner face of the liquid lens window, see. section 6.3.

5.4 Wave-front error requirement for OIS systems

With a camera featuring no OIS function, a handshake tilt with an amplitude of θ_{hs} will transform a sharp object point into a blurry image spot line with an amplitude of dr_{hs} as follow:

$$dr_{hs} = f \cdot \theta_{hs} \qquad (13)$$

Where f is the focal length of the camera lens. The OIS function enables to reduce the blur image down to a residual blur amplitude $dr_{residual\text{-}OIS}$:

$$dr_{residual-ois} = \frac{dr_{hs}}{BRF} \qquad (14)$$

where *BRF* is the blur reduction factor, characterizing the performances of the OIS system[10]. We have given in the previous section a rule of thumb for the evaluation of the wave-front error requirement of a camera lens so as to perform images with a resolution smaller than a pixel. A similar evaluation of the wave-front error requirement in OIS mode can be performed assuming that an OIS lens should perform images with a resolution smaller the residual image blur during a tilt. We can provide an approximate evaluation of this condition based on the following extrapolation of the Maréchal criterion:

$$WFE_{lens-rms} < \frac{\lambda}{14} \cdot \frac{dr_{residual-OIS}}{f \cdot \lambda / D} \qquad (14)$$

This expression gives a simple rule of thumb evaluation of the acceptable WFE of the OIS camera lens as a function of the optical tilt θ_{opt} generated by the system:

$$WFE_{lens-rms} < \frac{D}{14} \cdot \frac{\theta_{opt}}{BRF} \qquad (15)$$

For example, with a +/-33° field, f/2.8 aperture and 1/3.2 inch sensor, the wave-front error requirement of an OIS camera module featuring a blur reduction factor of 4 is 50nm/0.1°. The A316S OIS liquid lens performances[9] are in line with this requirement.

6. EXAMPLES OF REFERENCE DESIGNS FOR OIS CAMERA MODULE

6.1 Introduction

We describe below two examples for the implementation of A316S OIS liquid lens in a camera module with a ¼ inch sensor. Those systems have been defined according to the design rules of the previous section so as to perform an image quality with a resolution of one pixel.

6.2 A316S added on a standard 1/4 inch sensor camera lens

Below is the example of a transformation of a 3.2Mpix, ¼ inch sensor fix focus camera module into an OIS/AF camera module. The A316S OIS liquid lens is plugged onto the camera module lens. The design presents no vignetting. The liquid lens provides a focus range from 5cm to infinite and a +/-0.6° tilt correction range for the OIS function.

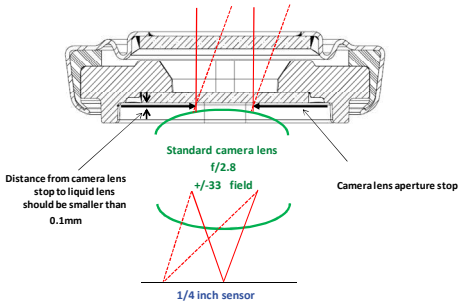

Figure 10. A316S on standard camera lens (f/2.8 – 1/4 inch sensor – 3.2Mpix – +/- 33° field).

6.3 A316S with intra-pupil added on a custom 1/4 inch sensor camera lens

We show in figure 11 the example of an AF/OIS camera module with a 5Mpix, ¼ inch sensor and f/2.8 aperture. The camera lens is specifically designed for a 1.25mm diameter intra-pupil positioned in the A316S liquid lens.

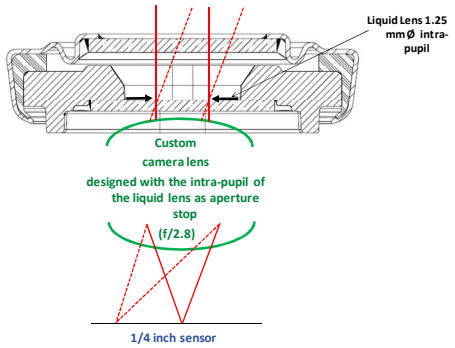

Figure 11. A316S on custom camera lens (f/2.8 – 1/4 inch sensor – 5Mpix – +/-33° field).

7. EXAMPLES OF APPLICATIONS FOR THE OIS LIQUID LENS

The OIS liquid lens is mainly dedicated to image stabilization for miniature camera modules. The electrical command of the optical power and of the optical tilt with a miniature component can also be used in a wide range of applications in optics. The main design rule when using a liquid lens is the limitation of the useful diameter of the liquid lens according to the optical wave-front error requirement for the lens operation in a given focus and tilt range. For imaging applications, the calculation principle of the maximal useful diameter of the liquid lens is described in section 5. For applications demanding diffraction limited optics, such as mono-mode laser optics, we use the Maréchal criterion. We give below possible examples of applications of the OIS liquid lens

7.1 Optical beam fine tuner

With a single OIS liquid lens it is possible to finely tune the tilt and divergence of a light beam. With 2 OIS liquid lenses separated with a spacer as described in figure 12, it is possible to finely tune the geometry of an optical light beam:

- The tilt of the light beam can be adjusted by a tilt command on one or both liquid lenses.
- The translation of the light beam along x-y axes can be obtained with an opposite tilt command on each lens.
- The divergence and size of the light beam can be tuned with a combination of the focus command of the 2 lenses.

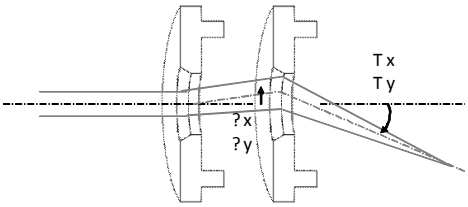

Figure 12. Optical beam fine tuner using 2 OIS liquid lenses for beam translation, tilt, size and divergence control

The optical beam fine tuner can be used for multiple optical setups demanding fine alignment such as laser cavity or optical coupling in an optical fiber. We present in figure 13 the principle of an automated system dedicated to optimize the light injected in an optical fiber. A simplified design featuring only one liquid lens for tilt control with a collimating lens is presented in figure 14.

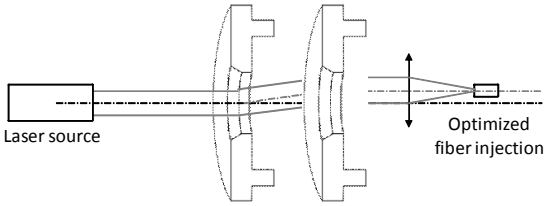

Figure 13. Optimized fiber injection using 2 OIS liquid lenses and a fiber collimation lens

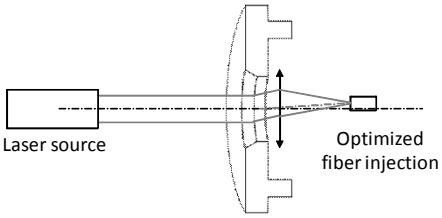

Figure 14. Optimized fiber injection using 1 OIS liquid lens and a fiber collimation lens

7.2 Tunable wavelength filter

The association of an OIS liquid lens with a passive component having a transmission depending on the incident angle of the light beam creates an active wavelength filter. We show in figure 15 below the optical scheme of an active wavelength filter based on the association of an OIS liquid lens and a diffractive grating. The transmission wavelength of the filter can be adjusted by θ_x tilt command on the liquid lens.

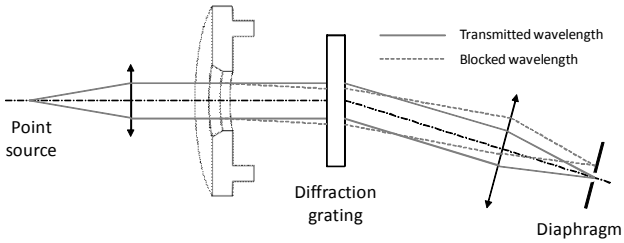

Figure 15. Wavelength selection with θ_x tilt command on an OIS liquid lens

7.3 Optical multiplexing

In the design shown in figure 16, two arrays of optical waveguides (input / output) are interconnected with two collimating lenses and two OIS liquid lenses. One of the light beams from the input array can be selected with a given x-y tilt command of the first OIS liquid lens, and coupled into one of the optical wave guides of the output array with another given x-y tilt command of the second OIS liquid lens.

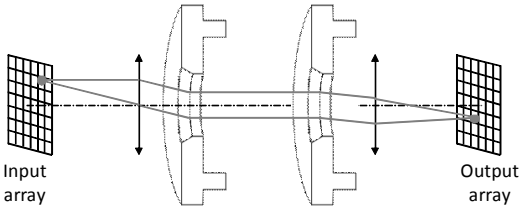

Figure 16. Optical multiplexing between 2 waveguide arrays using 2 OIS liquid lenses

8. CONCLUSION

We have presented the principle, the driving method and the performances of our A316S OIS liquid lens component. We have explained optical design rules for the implementation of the liquid lens in optical systems and we have shown different possible application designs. The A316S component is silent, robust and easy to integrate. It can combine OIS and smooth AF for picture and video with low electrical consumption. The current reliability features obtained today- 1 million AF/OIS cycles from -10°C to 60°C and 120h at 85°C storage - are being improved to keep up with the most severe mobile phone reliability requirements.

9. ACKNOWLEDGEMENT

The authors would like to thank Nelly Garcia-Jaldon, Ly Pich, Géraldine Malet, Nicolas Samper, Jérôme Broutin and Florent Thieblemont for their support in the development of the OIS liquid lens. We also thank our student Ludivine Bruyère who performed experimental evaluation of the algorithms for tilt response time optimization

REFERENCES

[1] Xiao, F., Farrell, J.E., Catrysse, P.B., Wandell, B., “Mobile Imaging: The Big Challenge of the Small Pixel,” Proc. SPIE 7250, 72500K (2009).
[2] Shimohata, T., Tsuchida, Y., Kusaka, H., “Control Technology for Optical Image Stabilization,” SMPTE journal 111, 609–615 (2002).
[3] Yu, H.C., Lee, T. Y., Wang, S. J., Lai, M. L., Ju, J. J., Huang, D. R., "Low power consumption focusing actuator for a mini video camera," J. Appl. Phys. 99, 08R901 (2006)
[4] Lippmann, G., “Relations entre les phénomènes électriques et capillaires,” Ann. Chim. Phys. 5, 494-549 (1875)
[5] Berge, B., “Electrocapillarité et mouillage de films isolants par l’eau,” C. R. Acad. Sci. Paris 317, 157-163 (1993)
[6] Berge, B., Peseux, J., “Variable focal lens controlled by an external voltage : An application of electrowetting,” J. Eur. Phys. J. E, 3(2), 159-163 (2000)
[7] Mugele, F. and Buehrle, J., “Equilibrium drop surface profiles in electric fields,” J. Phys. Condens. Matter, 19 375112 (2007)
[8] Maillard M. , Legrand J. Berge B., “Two Liquids Wetting and Low Hysteresis Electrowetting on Dielectric Applications,” *Langmuir, 25* (11), 6162–6167 (2009)
[9] Simon, E., Craen, P., Gaton, H., Jacques-Sermet, O., Laune, F., Legrand, J., Maillard, M., Tallaron, N., Verplanck, N. and Berge, B. "Liquid lens enabling real-time focus and tilt compensation for optical image stabilization in camera modules," Proc. SPIE 7716, 77160I (2010).
[10] Simon, E., Berge, B., Gaton, H., Jacques-Sermet, O., Laune, F., Legrand, J., Maillard, M., Moine, D. and Verplanck, N., “Optical image stabilization with a liquid lens,” to be published in Proc. ODF Yokohama, (2010)
[11] Born and Wolf, [Principles of Optics], Oxford Pergamon, (1970)
[12] Maréchal, A., PhD Thesis "Etude des influences conjuguées des aberrations et de la diffraction sur l’image d’un point, “ Faculté des Sciences de Paris, (1947).
[13] Yotam, E., Ephi, P., and Ami, Y., “MTF for Bayer pattern color detector,” Proc. SPIE 6567, 65671M (2007).